Journal of Sound and Vibration (1991) **148**(1), 1-9

AN EXAMINATION OF MULTI-FREQUENCY EXCITATION OF THE BUCKLED BEAM

C. PEZESHKI, S. ELGAR†† AND R. C. KRISHNA

Department of Mechanical and Materials Engineering, Washington State University, Pullman, Washington 99164-2920, *U.S.A.*

(*Received* 14 *November* 1989)

The dynamics of a magnetically buckled beam excited by a two-frequency forcing function are examined to determine the nature and cause of the system behavior into and outside the parameter range where chaotic oscillations are observed. To facilitate the analysis, the beam is modelled by Duffing's equation with a negative linear stiffness. Bispectral analysis is performed on the trajectories in order to examine the nature and effect of frequency coupling in the motion. Results indicate that varying the relative phase angle of the higher frequency term can result in driving the system in and out of chaos. Bispectral analysis indicates that this controlling behavior of the high-frequency excitation term can be explained by quadratic interactions that transfer energy to the lowest non-linear natural frequency of the beam.

1. INTRODUCTION

The magnetically buckled beam has been studied by a variety of authors (see references [1, 2] and references therein), and behavior for the one spatial mode Galerkin reduction of the beam, otherwise known as Duffing's equation with a negative linear stiffness is well documented. The beam's motion is described by

$$\ddot{A} + \gamma \dot{A} - \tfrac{1}{2}(A - A^3) = F_0 \sin \Omega t, \tag{1}$$

where A is the displacement at the tip of the beam, γ is the sampling coefficient, the excitation force has amplitude F_0 and frequency Ω, and the overdot represents differentiation with respect to time. Duffing's equation and the buckled beam exhibit phenomena such as period doubling and chaotic oscillations.

The magnetically buckled beam is often referred to as a two-well potential problem. At rest, the physical system has two stable equilibria, one buckled about the left magnet, the other about the right magnet (see Figure 1). The beam also has one unstable equilibrium, located about the center of the two magnets. If excited with a small sinusoidal force, the beam will oscillate about one of the two stable equilibria in a roughly sinusoidal fashion. However, when the force amplitude is raised to a sufficient level, the beam will jump back and forth between the two static equilibria, in effect "snapping through" the centerline of the system.

The purpose of the present study is to demonstrate the effect of supplemental forcing terms on the global behavior of the magnetically buckled beam system. Since the system is non-linear, the effects of these terms cannot be calculated readily by the method of superposition.

† With the Department of Electrical and Computer Engineering, Washington State University.

0022-460X/91/130001+09 $03.00/0

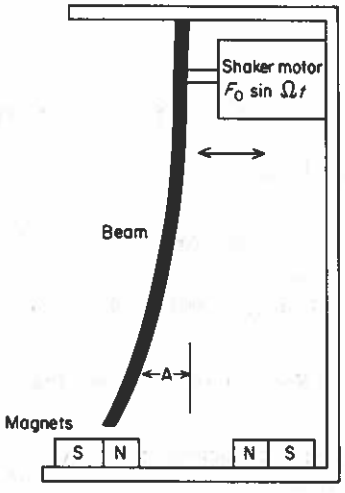

Figure 1. The magnetically buckled beam.

Two illustrative cases were analyzed, represented by the following equations:

$$\ddot{A} + \gamma \dot{A} - \tfrac{1}{2}(A - A^3) = F_0 \sin \Omega t + F_0 \sin (2\Omega t + \varphi), \tag{2}$$

$$\ddot{A} + \gamma \dot{A} - \tfrac{1}{2}(A - A^3) = F_0 \sin \Omega_0 t + F_0 \sin \Omega_1 t. \tag{3}$$

Systems with cubic non-linearities, including some with two-frequency excitation, have been investigated previously (see references [3, 4] and references therein). The present study is an investigation of methods of quenching chaotic motion by varying the phase angle, φ, of the forcing term in equation (2). A non-linear frequency response equivalent of the system is determined from equation (3).

In order to obtain results that can be compared with previous work, parameter values for the above equations were the same as values used in reference [2], in particular, the damping value, $\gamma = 0{\cdot}168$. A period doubling sequence into and out of chaos for equations (2) and (3) was observed. For equation (2), the phase angle φ was varied and the system was observed in the chaotic regime. For equation (3), as the force amplitude F_0 was raised, the system typically underwent a period doubling cascade, followed by an intermittency crisis, as was also observed for equation (1) in reference [2]. Auto-bicoherences were then calculated for the trajectories, and intuitive conclusions were reached by examining these bicoherences.

Relevant bispectral quantities are defined and details of the numerics are presented in the next section. Results of numerical integrations of equations (2) and (3), including power and bicoherence spectra and phase plane analysis are presented in section 3. Conclusions follow in section 4.

2. BISPECTRAL ANALYSIS AND NUMERICAL DETAILS

Details and applications of bispectral analysis can be found in references [5–8]. A brief description is presented here for completeness.

For a discretely sampled time series $\eta(t)$ with the Fourier representation

$$\eta(t) = \sum_n C(\omega_n)\, e^{i\omega_n t} + C^*(\omega_n)\, e^{-i\omega_n t}, \tag{4}$$

the power, auto- and the cross-bicoherence spectra (normalized bispectra), are defined respectively as

$$P(\omega) = \mathrm{E}[C(\omega)C^*(\omega)], \tag{5}$$

$$B(\omega_1, \omega_2) = \mathrm{E}[C(\omega_1)C(\omega_2)C^*(\omega_1+\omega_2)]/P(\omega_1)P(\omega_2)P(\omega_1+\omega_2), \tag{6}$$

$$XB_{j,k}(\omega_1, \omega_2) = \mathrm{E}[C_j(\omega_1)C_j(\omega_2)C_k^*(\omega_1+\omega_2)]/P_j(\omega_1)P_j(\omega_2)P_k(\omega_1+\omega_2), \tag{7}$$

where ω_n is the radian frequency, the subscript n is a frequency index, the Cs are the complex Fourier coefficients of the time series, an asterisk indicates complex conjugate, and E[ ] is the expected-value, or average, operator. The subscripts j, k in equation (7) indicate separate time series; in the cases considered here, input and output, respectively. Upon rewriting the complex Fourier coefficients as $C(\omega_n) = c_n\, e^{i\Phi_n}$, the bispectrum becomes

$$B(\omega_1, \omega_2) = \mathrm{E}[c_1 c_2 c_{1+2}\, e^{i(\Phi_1+\Phi_2-\Phi_{1+2})}]. \tag{8}$$

If the three modes of the triad are independent of each other (i.e., Φ_1, Φ_2 and Φ_{1+2} are random phases), then when averaged over many realizations the triple products in equations (6–8) will be zero. On the other hand, if the modes at frequencies ω_1, ω_2 and $\omega_1+\omega_2$ are quadratically coupled, the biphase $(\Phi_1+\Phi_2-\Phi_{1+2})$ will be non-random even if Φ_1 and Φ_2 are randomly varying. Thus, the bispectrum will be non-zero. Consequently, the bicoherence indicates the relative amount of quadratic phase coupling between the three modes in a triad.

3. RESULTS

For many weakly non-linear systems, non-linear resonances are often observed at the linearized natural frequency and at twice the natural frequency [9]. Consequently, equation (2) with $\Omega = 0{\cdot}159$ Hz, the first resonance of the system, was examined. F_0 was set at 0·21, the chaos boundary at which chaotic oscillations are first observed for the single-frequency excitation case [2]. The phase plane trajectories for $\varphi = 0{\cdot}0$, 0·20, 0·28, 0·31, 0·32 and 0·50 in Figure 2. Varying the phase angle for this forcing function produces a classic period doubling sequence (Figures 2(f)–2(c)), followed by an intermittency crisis into and out of chaos. The period doubling sequence into chaos is almost identical to the single-frequency forcing case; see reference [2] for comparison. Power spectra for the respective attractors are shown in Figure 3. As expected, for the power spectra shown in Figure 3(a) and 3(e), a strong subharmonic is present at half the excitation frequency. The power spectrum shown in Figure 3(b) is broadband, typical of a chaotic system, and the power spectra shown in Figures 3(c) and 3(d) contain the requisite subharmonics for period octupling and period quadrupling.

Auto-bicoherences for the system are presented in Figure 4. Quadratic behavior is pre-eminent. Strong peaks in the bicoherence are prevalent at triads that include the driving frequency ($f = 0{\cdot}159$ Hz) and its sub- and superharmonics ($f_1 = 0{\cdot}159$ Hz, $f_2 = 0{\cdot}159$ Hz, $f_{1+2} = 0{\cdot}318$ Hz), ($f_1 = 0{\cdot}0795$ Hz, $f_2 = 0{\cdot}0795$ Hz, $f_{1+2} = 0{\cdot}159$ Hz), and ($f_1 = 0{\cdot}159$ Hz, $f_2 = 0{\cdot}0795$ Hz, $f_{1+2} = 0{\cdot}2385$ Hz) in Figures 4(a), (c), (d) and (e). The system's bicoherences are almost identical to the case of single-frequency forcing [10]. There is little quantitative difference between the bicoherences of the single-frequency excitation period 1, 2, 4 and chaotic attractors and the period 1, 2, 4 and chaotic attractors generated by equation (2).

The cross-bicoherence of the input signal relative to the output (Figure 5) for a single-period limit cycle (i.e., Figures 2(f), 3(f) and 4(f)) shows a mechanism that is consistent with the control frequency transferring energy back to the natural frequency,

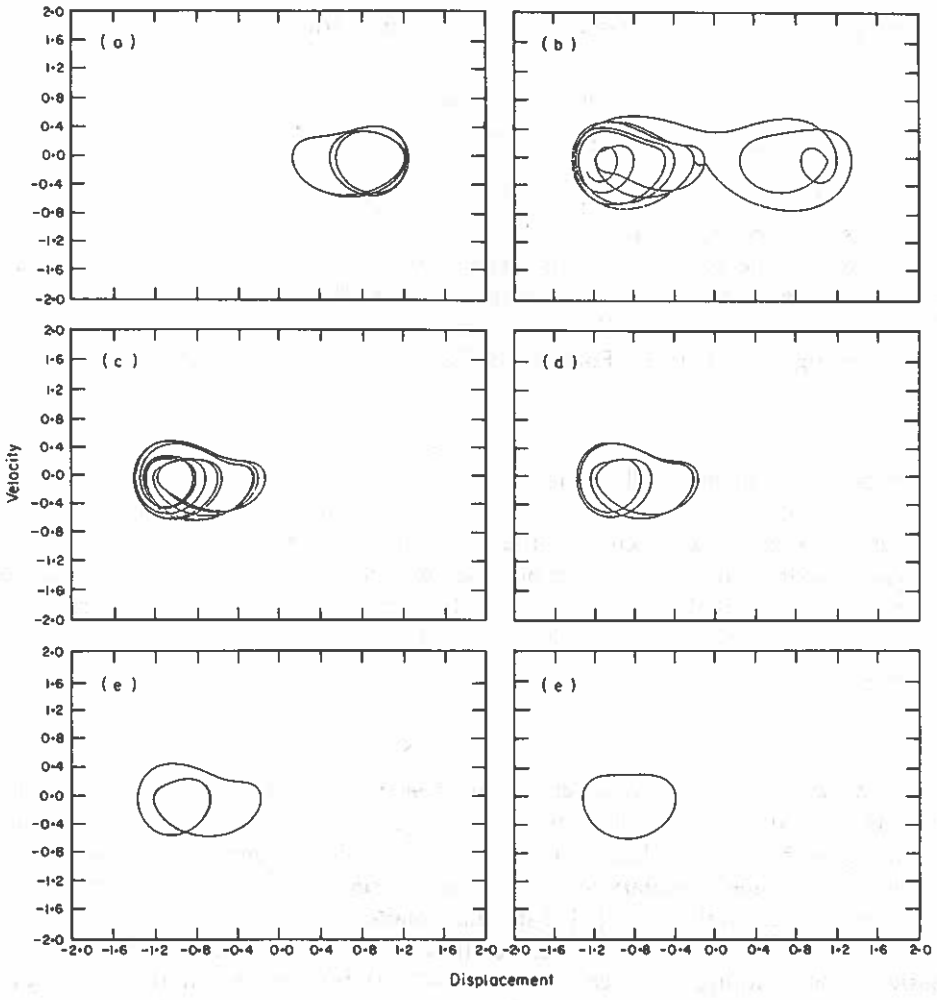

Figure 2. Phase plane trajectories, equations (2); $F_0 = 0{\cdot}21$; $\Omega_1 = 1$, $\Omega_2 = 2$; $\varphi =$ (a) 0·0, (b) 0·2, (c) 0·28, (d) 0·31, (e) 0·32 and (f) 0·5.

which then redistributes the energy between the harmonics as it had done with the single-frequency excitation case [10]. A summing interaction is found between $f = 0{\cdot}159$ Hz, the excitation at the natural frequency, and itself, creating the frequency triad ($f_1 = 0{\cdot}159$ Hz, $f_2 = 0{\cdot}159$ Hz, $f_{1+2} = 0{\cdot}318$ Hz). A differencing interaction is found between the controlling frequency, $f = 0{\cdot}32$ Hz, and the main excitation, $f = 0{\cdot}159$ Hz, creating the frequency triad ($f_1 = 0{\cdot}318$ Hz, $f_2 = 0{\cdot}159$ Hz, $f_{1-2} = 0{\cdot}159$ Hz). By varying the phase of the controlling frequency input, an effect is observed whereby the phase of the frequency generated by the differencing interaction between ($f_1 = 0{\cdot}318$ Hz, $f_2 = 0{\cdot}159$ Hz, $f_{1-2} = 0{\cdot}159$ Hz) effectively creates an out-of-phase motion between $f_{1-2} = 0{\cdot}159$ Hz and the main excitation, also at $f = 0{\cdot}159$ Hz. This interaction thus enables quenching of the chaotic motion to occur by effectively raising or lowering F_0 for the main sinusoidal input. Cases were also run with the phase angle equal to $0{\cdot}85\pi$ and π (not shown). Maximum quenching was observed at $0{\cdot}85\pi$. The slight phase angle shift from the maximum out-of-phase effect is attributed to the cubic behavior of the system. This offers possibilities for the control of non-linear systems with strong harmonic content by imposing oscillations at frequencies other than the primary.

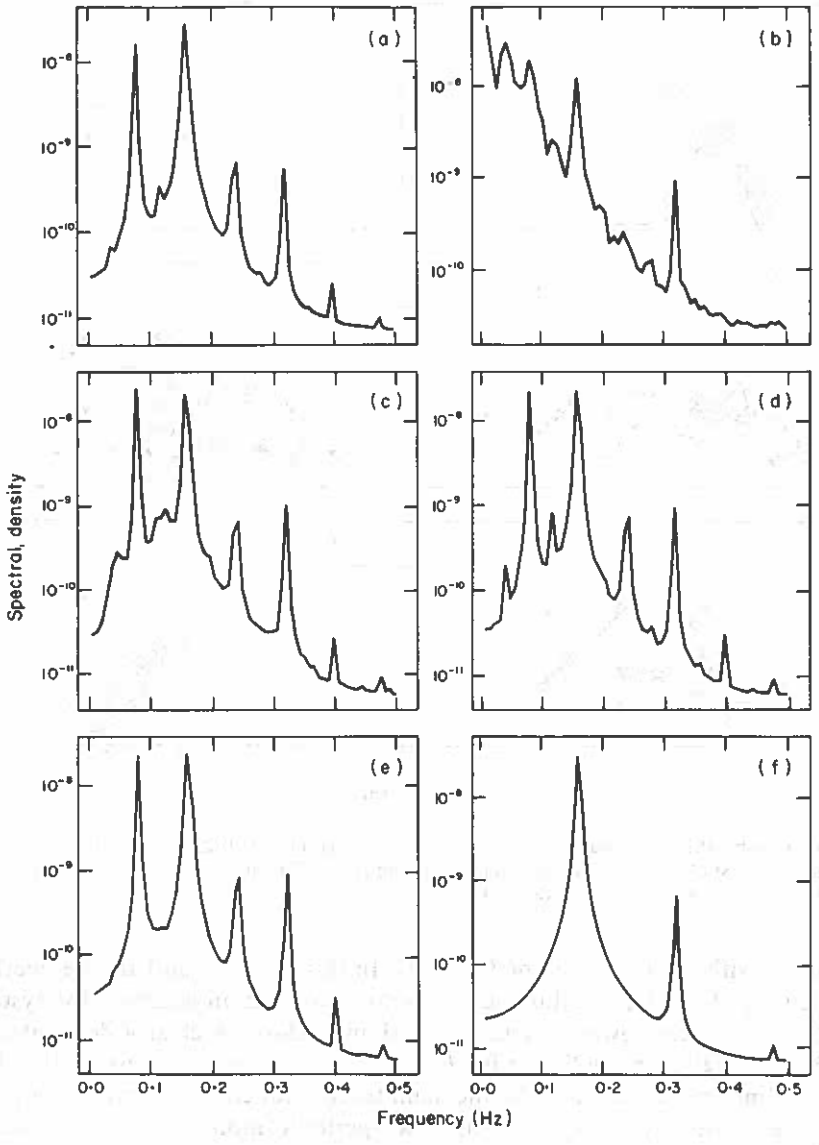

Figure 3. Power spectra, equation (2); $F_0 = 0{\cdot}21$; φ = (a) 0·0, (b) 0·2, (c) 0·28, (d) 0·31, (e) 0·32 and (f) 0·5. The units of power are arbitrary.

Once the system makes the transition to the chaotic regime, bicoherence spectra (Figure 4(b)) indicate very little quadratic coupling. This is because the system, the motion of which in the chaotic regime spans the entire phase space, exhibits primarily cubic behavior, since the dominant non-linearity is cubic. Thus, the bicoherence is of only limited value for analyzing this particular system in the chaotic regime.

The behavior of equation (3) was considered by setting Ω_0 equal to the linearized natural frequency of the system, $\Omega_0 = 0{\cdot}159$ Hz, while Ω_1 was varied at 1·7 times (0·27 Hz), twice (0·318 Hz) and four times Ω_0 (0·636 Hz). A period doubling sequence leading into chaos was observed for each of the frequency combinations except for $\Omega_1 = 0{\cdot}27$ Hz.

Phase portraits for the frequency combinations into chaos showed little difference between the single frequency excitation [2] and the multi-frequency excitation used in

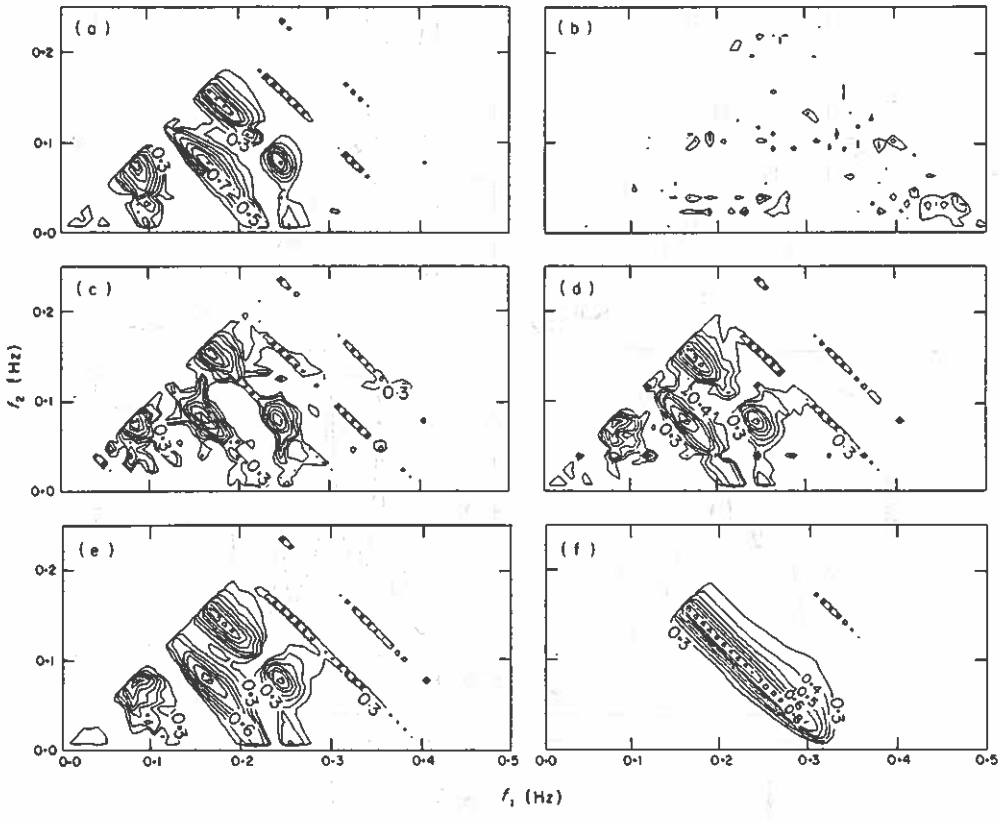

Figure 4. Auto-bicoherences, equation (2); $F_0 = 0{\cdot}21$; $\varphi =$ (a) 0·0, (b) 0·2, (c) 0·28, (d) 0·31, (e) 0·32 and (f) 0·5. Triads consist of modes with frequencies f_1, f_2 and $f_1 + f_2$. The minimum contour shown is $B = 0{\cdot}3$, the 95% significance level, with contours every 0·1.

equation (3), with the exception of $\Omega_1 = 0{\cdot}27$. In this case, Ω_0 and Ω_1 are nearly incommensurate ($\Omega_0/\Omega_1 \simeq \sqrt{3}$), and thus a quasi-periodic oscillation occurs in the system below chaos (Figure 6). The power spectrum (not shown) shows a clearly delineated spike at $f = 0{\cdot}159$ Hz as well as $f \times 0{\cdot}270$ Hz for F_0 well below the value necessary for chaos. The steady state limit cycle generated by the main forcing function is perturbed by a force at an incommensurate frequency, causing quasi-periodic motion, similar to that for the sinusoidally forced Van der Pol equation.

Auto-bicoherence spectra (not shown) for the cases where the control frequency was an integer multiple of the natural frequency were similar to those for equation (2). The only effect of adding an excitation at one of the frequencies automatically generated by the system through quadratic interaction was to vary the phase portrait shape by a minor amount and add more energy to the power spectrum at the frequency. The cross-bicoherence between input and output for $\Omega_0 = 0{\cdot}159$ Hz, $\Omega_1 = 0{\cdot}636$ Hz (Figure 8) indicates that the same summing and differencing interactions occur. The main input excitation interacts with itself in the triad ($f_1 = 0{\cdot}159$ Hz, $f_2 = 0{\cdot}159$ Hz, $f_{1+2} = 0{\cdot}318$ Hz), while the control frequency interacts with the main frequency for a frequency differencing effect ($f_1 = 0{\cdot}636$ Hz, $f_2 = 0{\cdot}159$ Hz, $f_{1-2} = 0{\cdot}477$ Hz). This similar behavior occurs even for the quasi-periodic oscillation (Figure 7).

As the higher frequency forcing term moves further away from the fundamental frequency of the system, interaction between the controlling and driving frequencies

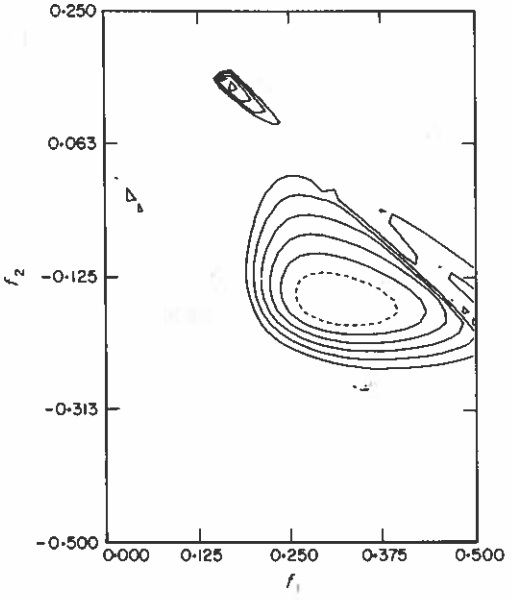

Figure 5. Cross-bicoherence between the forcing function (f_1, f_2) and displacement (f_1+f_2) corresponding to Figures 2(f), 3(f) and 4(f). The minimum contour plotted is $XB=0{\cdot}4$, with contours every 0·1. ($F_0=0{\cdot}21$, $\varphi=0{\cdot}5$.)

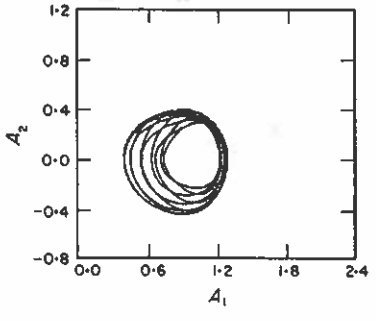

Figure 6. Quasi-periodic limit cycle, equation (3); $\Omega_0=0{\cdot}159$ Hz, $\Omega_1=0{\cdot}270$ Hz; $F_0=0{\cdot}10$.

diminishes, as can be seen by comparing Figures 4, 7 and 8, the cross-bicoherences between input and output for the excitation cases ($\Omega_0=0{\cdot}159$ Hz, $\Omega_1=0{\cdot}318$ Hz), ($\Omega_0=0{\cdot}159$ Hz, $\Omega_1=0{\cdot}270$ Hz) and ($\Omega_0=0{\cdot}159$ Hz, $\Omega_1=0{\cdot}636$ Hz) respectively. For Figure 5, the cross-bicoherence value for the triad ($f_1=0{\cdot}318$ Hz, $f_2=0{\cdot}159$ Hz, $f_{1-2}=0{\cdot}159$ Hz) is $XB=0{\cdot}9$. For Figure 7, the cross-bicoherence value for the triad ($f_1=0{\cdot}270$ Hz, $f_2=0{\cdot}159$ Hz, $f_{1+2}=0{\cdot}111$ Hz) is $XB=0{\cdot}9$. For the case shown in Figure 8, the cross-bicoherence value for the triad ($f_1=0{\cdot}636$ Hz, $f_2=0{\cdot}159$ Hz, $f_{1-2}=0{\cdot}477$ Hz) is only $XB=0{\cdot}5$. As the system is driven by excitations further away from the fundamental frequency, the behavior of the system, in a sense, becomes more linear for the same amplitude of the controlling force because the degree of non-linear interaction decreases.

The physical behavior of the beam confirms the validity of these results. Preliminary observation of the system in the laboratory indicates that if the beam is excited at a frequency other than the natural frequency of the system, energy is transferred to the dominant natural mode. Once the system is excited by a higher frequency force, with an

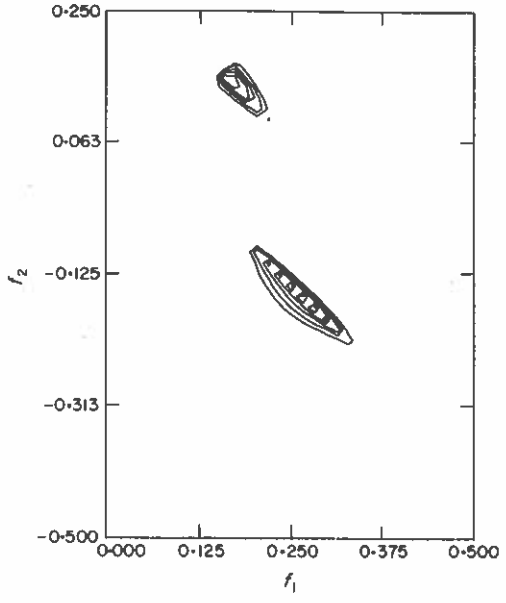

Figure 7. Cross-bicoherence between forcing function and displacement, equation (3); $F_0 = 0{\cdot}15$; $\Omega_0 = 0{\cdot}159$ Hz, $\Omega_1 = 0{\cdot}270$ Hz. The format is the same as Figure 5.

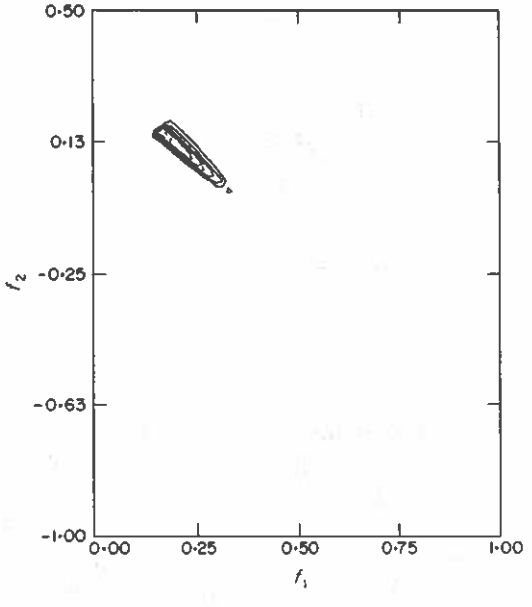

Figure 8. Cross-bicoherence between forcing function and displacement, equation (3); $F_0 = 0{\cdot}15$; $\Omega_0 = 0{\cdot}159$ Hz, $\Omega_1 = 0{\cdot}636$ Hz. The format is the same as Figure 5.

amplitude past the range of linear response, large-amplitude limit cycle or chaotic motion always occurs, with the same fundamental characteristic as if the system were excited at the linearized natural frequency. Although the system will respond at that particular excitation frequency, most of the excitation energy is transferred to the lower mode.

4. CONCLUSIONS

The effects of multi-frequency forcing for Duffing's equation were considered. Control of chaos, including its elimination and the restoration of periodic oscillations, was shown to be possible by varying the phase angle of a secondary sinusoid. Bispectral analysis techniques allowed the different motions to be separated into distinct, non-linear modes of vibration. Lower excitation frequencies, occurring near the natural resonances of the system, were shown to cause most of the non-linear effects; higher frequencies, further away from resonance, were shown to transfer energy back down to the fundamental modes through difference interactions. This offers novel methods of control for non-linear systems.

ACKNOWLEDGMENTS

Charles Pezeshki's work was supported by an internal Washington State University grant. Steve Elgar's research is supported by the Coastal Sciences Branch of the Office of Naval Research (N00014-86-K-0877) and the Physical Oceanography Program of the National Science Foundation (OCE-8612008). Signal processing computations were performed at the San Diego Supercomputer Center (supported by NSF). The authors thank D. L. Kinzer for help with the figures.

REFERENCES

1. F. C. MOON and P. J. HOLMES 1979 *Journal of Sound and Vibration* **38**, 275–296. A magneto-elastic strange attractor.
2. E. H. DOWELL and C. PEZESHKI 1986 *American Society of Mechanical Engineers Journal of Applied Mechanics* **53**(1), 5–9. On the understanding of chaos in Duffing's equation including a comparison with experiment.
3. R. H. PLAUT, N. HAQUANG and D. T. MOOK 1986 *Journal of Sound and Vibration* **107**, 309–319. The influence of an internal resonance on non-linear structural vibrations under two-frequency excitation.
4. L. D. ZAVODNEY, A. H. NAYFEH and N. E. SANCHEZ 1989 *Journal of Sound and Vibration* **129**, 417–442. The response of a single-degree of freedom system with quadratic and cubic non-linearities to a principal parametric resonance.
5. K. HASSLEMAN, W. MUNK and G. MACDONALD 1963 in *Time Series Analysis* (M. Rosenblatt, editor), 125–139. New York: John Wiley. Bispectra of ocean waves.
6. Y. C. KIM and E. J. POWERS 1979 *Institute of Electrical and Electronic Engineers Transactions on Plasma Science* **PS-7**(2), 120–131. Digital bispectral analysis and its applications to nonlinear wave interactions.
7. C. L. NIKIAS and M. R. RAGHUVEER 1987 *Institute of Electrical and Electronic Engineers Proceedings* **75**(7), 869–891. Bispectrum estimation: a digital signal processing framework.
8. R. A. HAUBRICH 1965 *Journal of Geophysical Research* **70**, 1415–1427. Earth noises, 5 to 500 millicycles per second, 1.
9. A. H. NAYFEH and D. T. MOOK 1979 *Nonlinear Oscillations* New York: John Wiley. See pp. 161–257 and references therein.
10. C. PEZESHKI, S. ELGAR and R. C. KRISHNA 1990 *Journal of Sound and Vibration* **137**(3), 357–368. Bispectral analysis of systems possessing chaotic motion.